Standalone Microgrid with Five-Level Diode Clamped Inverter Based Hybrid Generation System

Het S. Bhalja,
Department of Electrical Engineering,
School of Technolgy,
Pandit Deendayal Petroleum University,
Gandhinagar, India
het.bmtee17@sot.pdpu.ac.in

Amit Vilas Sant,
Department of Electrical Engineering,
School of Technolgy,
Pandit Deendayal Petroleum University,
Gandhinagar, India
amit.sant@sot.pdpu.ac.in

Anilkumar Markana
Department of Electrical Engineering,
School of Technolgy,
Pandit Deendayal Petroleum University,
Gandhinagar, India
anil.markana@spt.pdpu.ac.in

Bhavesh R. Bhalja
Department of Electrical Engineering,
Indian Institute of Technology
Roorkee,
India
brb14fee@iitr.ac.in

***Abstract*—This paper presents a new architecture for standalone microgrids incorporating 5-level diode clamped inverter (DCI) for interfacing hybrid generation system (HGS) with *ac* loads. The HGS involves photovoltaic (PV) arrays, battery packs and diesel generator (DG) that act as individual dc sources for DCI which in turn eliminates the need of input capacitors for DCI and the associated voltage balancing. For the DCI output voltage level of $2V_{dc}$, the DG and the combination of PV array and/or battery supply the load. Similarly, the PV array and/or battery feed the load when the voltage level is V_{dc}. Likewise, for the levels $-V_{dc}$ and $-2V_{dc}$, a separate PV array, battery pack and DG are operated in similar manner. In case the PV power is greater than the demand, it can be used to charge the battery. Conversely, if the PV power cannot meet the demand, then the charged battery pack can assist to feed the load. The system reliability and self-sustenance capability is enhanced with the use of DG. Additionally, as no synchronization with the DG is required, the need of fundamental current extraction is eliminated. The operation of the proposed standalone microgrids with 5-level DCI based HGS is analysed for different operating conditions.**

Keywords—Diesel generation, diode clamped inverters, microgrids, multilevel inverters, solar photovoltaic system

I. INTRODUCTION

Microgrids involve management of the energy supply for the localized loads with the help of localized distributed generation [1]. With the maturity of renewable energy technology and its wide acceptance, microgrids are not only expected to play significant in electric power generation for the electrified areas but also in the un-electrified rural areas [1]. Generally, villages are dispersed, have low population count, and are remotely located. Often this results in these locations remaining un-electrified due to geographical, technical and/or economic issues. For rural population, the availability of electric power can improve the standard of living and significantly enhance the prospects for economic growth [2]. In India, this has resulted in initiation of various government programs to bring the rural population under the ambit of electrification.

The advancements in and signal electronics has resulted in extensive usage of power converters leading to commercial viability and wider acceptance of the renewable energy technology [3], [4]. Renewable energy sources can be utilized to generate electric power to feed the localized load. Such an arrangement for localized small scale generation, distribution and consumption of electric power without the involvement of utility network while involving power electronic converters can be termed as standalone microgrid. In tropical region, solar energy, due to its free, clean and abundant availability [3], has emerged as one of the prime power source for the micorgrids. In spite of its numerous advantages and wide acceptance, it has a major demerit in terms of its unpredictable nature [5]. Due to this demerit, it cannot be relied upon to provide uninterrupted power supply [6]. Hence, provision of battery back-up, in spite of its high cost, is widely reported to support PV system in order to provide uninterruptible power supply [6-12]. Usually, multiple energy sources (renewable and conventional) and energy storage devices (ESDs) are involved in microgrids [1]. This results in hybrid generation system (HGS). Blackstone et al have stated that diesel generator (DG) needs to be employed for practical and reliable microgrids, as it can cater to the load demand in the absence of the renewable energy supply [1]. For standalone microgrids operating in un-electrified areas, DGs are an ideal energy source as they can offer the merits of increased power reliability, self-sustenance and freedom from dependence on atmospheric conditions. References [5, 8-12] have reported the use of DG in microgrids.

In the power structure of standalone microgrids, power electronic converters (PECs) serve as an interface between the multiple energy sources, ESDs and localized loads to ensure the optimal control of unidirectional and bidirectional flow of power flow, while respecting the specifications of load, energy sources and ESDs. Each of the energy sources and ESDs are connected to an individual PEC (which can be a dc-dc converter or rectifier) that supplies the load through a common voltage source inverter (VSI). 2-level VSIs are reported in isolated microgrids feeding *ac* loads [1, 10, 12]. Multi-level inverters (MLIs) can be preferred over two level inverters due to its advantages of lower distortion in output voltage, reduced *dv/dt* and voltage stress, improved power quality at supply end, reduced common mode voltages, etc [13]. A survey of different MLI topologies is reported by Rodriguez et al [13]. Among these topologies, DCI offers advantage over the cascade topology in terms of lower switch count, reduced size, higher efficiency [13-14]. References [15-16] have presented PV array feeding the load from a single PV array through a DCI.

This paper proposes a new configuration for standalone microgrid wherein a 5-level DCI is employed to interface the

978-1-5386-8158-9/19/$31.00 ©2019 IEEE

HGS (comprising of PV, battery pack and DG) with the *ac* load. Novelty of this topology is that instead of a single dc-link feeding the inverter, each source and ESD is interfaced with DCI. The output voltage levels of DCI, ie. 0, +/-V_{dc}, and +/-$2V_{dc}$ is either due to the energy source or ESD or series combination of (i) two energy sources, (ii) two ESDs, or (iii) energy source and ESD. This results in elimination of the need of input capacitors for DCI and the associated voltage balancing. In addition to this, the use of MLI ensures that the power quality is significantly improved at the output and voltage stress on the switches is reduced. Furthermore, the incorporation of DGs as an energy source enhances the system reliability and provides self-sustenance capability. In conventional microgrids the synchronization of energy sources with DG is mandated. However, in proposed topology no synchronization with the DG and as a consequence no fundamental current estimation is required. The operation of proposed standalone microgrid with 5-level DCI based HGS is demonstrated for five different operating conditions.

II. Standalone Microgrid Architecture

Fig. 1 shows a general architecture of a standalone microgrid comprising of HGS, where V_{pv}, V_{bat} and V_{dg} are the terminal voltages of PV array, battery pack and DG, I_{pv}, I_{inv} and I_{dg} are the currents supplied by PV array, VSI and DG, P_{pv}, P_{bat} and P_{dg} are the powers supplied by the PV array, battery pack and DG, V_{dc} is the *dc*-link voltage, and C_{dc} is the *dc*-link capacitor. Standalone microgrid comprises of PV panel as an energy source interfaced with the *dc* link through a *dc-dc* converter. This converter controls the flow of power from PV array to the load while ensuring that the PV operation at the maximum power point. Battery pack is employed as an energy storage element interfaced with the common *dc* bus through the bidirectional *dc-dc* converter. This converter ensures controlled charging and discharging of the battery. VSI, connected in parallel with the DG at G_1-G_2, needs to be synchronized with the DG. Also, the VSI is operated in current controlled mode so that I_{inv} is in phase with the fundamental active component of I_{dg}. This necessitates fundamental current extraction algorithm.

During the day time, the PV panel can cater to the load demand. If the PV power is insufficient to meet the load demand then the battery or DG can assist the PV to meet the load demand. Firstly, the battery needs to supply power to meet the demand. If battery is discharged or unable to supply the power so as to meet the demand, then the DG would come into the picture to supply the load. Alternately, if the PV power exceeds the load demand then the excess power can be used to charge the battery. If the battery is fully charged then the excess power needs to be dissipated in the dummy load. In this scenario, DG remains in idle state and need not be operated.

During the periods of low light intensity, such as night time, the PV panel plays no role in the power generation. The charged battery can feed the load through the bidirectional dc-dc converter and VSI. If at all the battery is unable to meet the load demand then DG provides the power to meet the load demand. DG gains prominence as a single energy source in case the battery is discharged. Thus, the use of DG ensures reliability and continuity of the electric power supply irrespective of the environmental conditions.

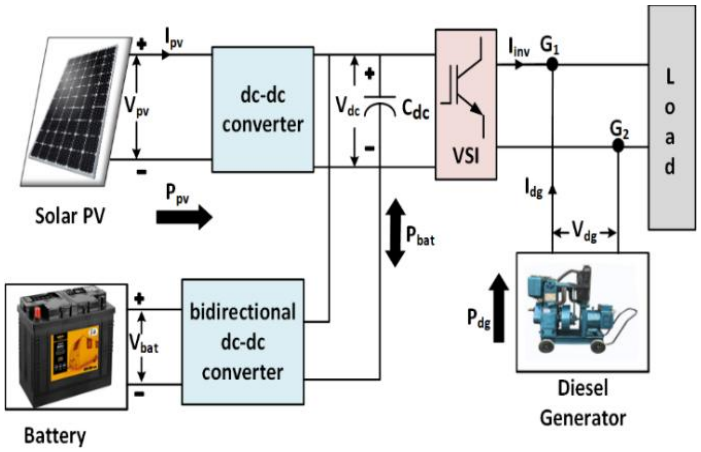

Fig. 1. General architecture of standalone microgrid with HGS.

III. Proposed Standalone Microgrid using DCI

Fig. 2 shows block diagram representation of the proposed 5-level DCI based HGS for standalone microgrid. In this system, HGS consists of (i) PV arrays (PV_1 and PV_2), (ii) battery packs (B_1 and B_2), and (iii) DGs (DG_1 and DG_2). PV_1 and B_1 are interfaced through individual *dc-dc* converters to form a common *dc*-link, whose voltage is regulated at V_{dc2}. B_1 required bidirectional *dc-dc* converter for the facilitation of controlled charging as well as discharging. Similarly, *dc*-link, with voltage level of V_{dc3}, is formed by interfacing PV_2 and B_2 through separate *dc-dc* converters. These two combinations of PV, battery pack and *dc-dc* converters are termed as $PVES_1$ and $PVES_2$. The *ac* voltages, V_{dg1} and V_{dg2}, generated by DG_1 and DG_2 undergo uncontrolled rectification to obtain *dc* voltages, V_{dc1} and V_{dc4}. Thus, V_{dc1}, V_{dc2}, V_{dc3} and V_{dc4} are made available as input voltages for the 5-level DCI, which ensures regulated *ac* supply for the load.

In the proposed topology, 5-level DCI comprises of six IGBTs (S_1-S_6) and four diodes (D_1-D_4). For an input supply voltage of V_d, the voltage across each input capacitor of the conventional 5-level DCI would be V_d/4.When operational, voltage balancing across the input capacitor is necessitated for the proper functioning. However, in proposed topology DG_1, $PVES_1$, $PVES_2$, and DG_2 are the four sources for 5-level DCI and hence, the need of voltage balancing is eliminated.

Table I shows the switching sequence of the 5-level DCI and the corresponding output voltage levels. V_{dc1}, V_{dc2}, V_{dc3} and V_{dc4} are regulated by means of *dc-dc* converters or field excitation control at V_{dc}. The output voltage of DCI can attain five levels (zero, $\pm V_{dc}$, and $\pm 2V_{dc}$) for the corresponding switching states, as indicated in Table I.

For the desired operation of proposed topology, input voltages to the 5-level DCI, V_{dc1}–V_{dc2}–V_{dc3}–V_{dc4}, need to be equal (i.e. $V_{dc1}=V_{dc2}=V_{dc3}=V_{dc4}=V_{dc}$). In order to ensure this, the automatic voltage regulation (AVR) system controls the field excitation of DG_1 and DG_2, resulting in $V_{dc1}=V_{dc4}=V_{dc}$. $PVES_1$ and $PVES_2$ regulate V_{dc2} and V_{dc3}, respectively. The duty cycles of *dc-dc* converters associated with $PVEC_1$ and $PVES_2$ are controlled so that V_{dc2} and V_{dc3} are regulated at V_{dc}. This leads to $V_{dc1}=V_{dc2}=V_{dc3}=V_{dc4}=V_{dc}$. $PVEC_1$ and $PVES_2$ is operate based on available PV power, load demand and battery pack capacity as discussed in Section-I. The charging and discharging of the battery pack are

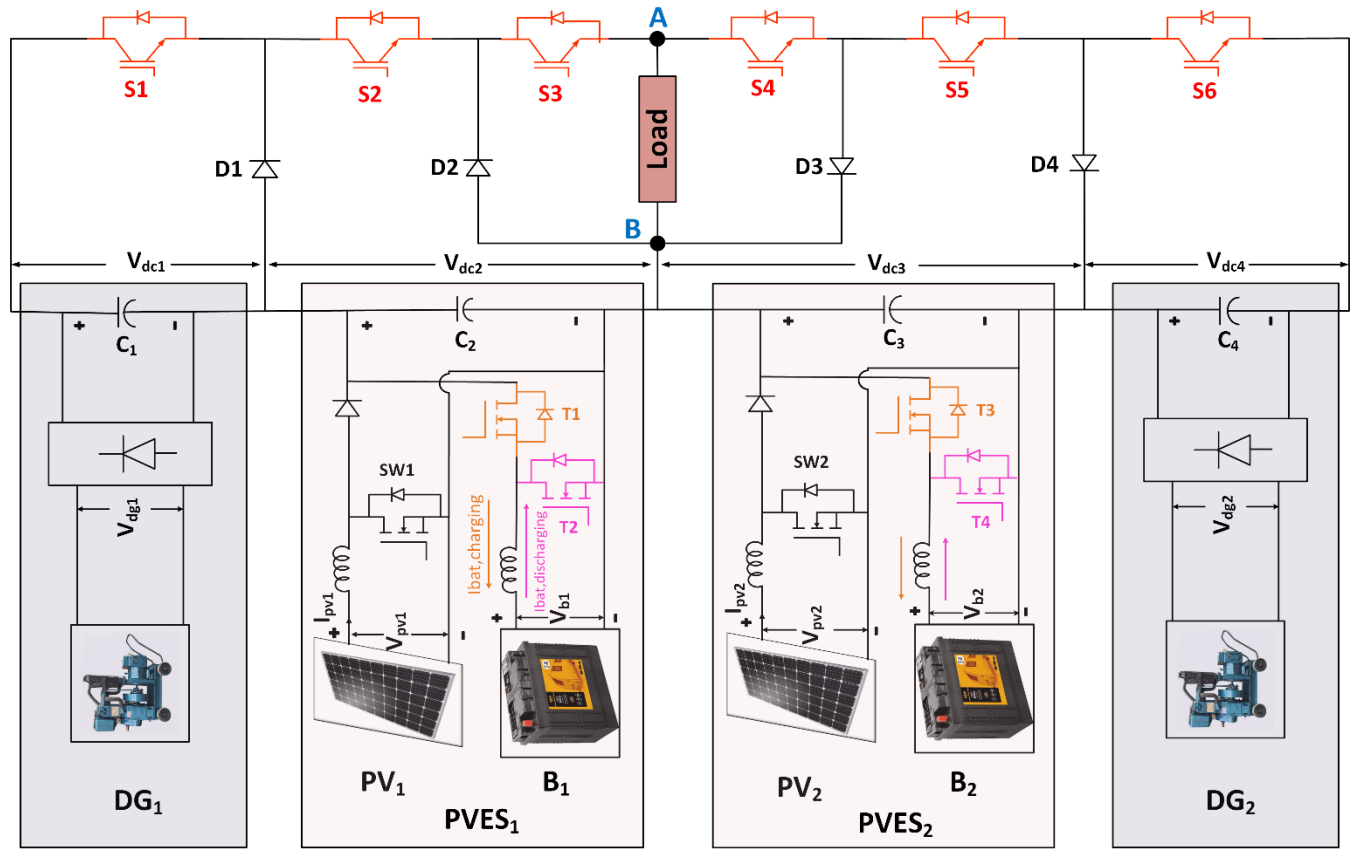

Fig. 2. Diagram of the proposed 5-level DCI based standalone microgrid

controlled by the bidirectional *dc-dc* converter. The details of mathematical modelling of PV cell, battery pack and 5-level DCI are provided in following sub-sections.

TABLE III. SWITCHING SEQUENCE OF 5-LEVEL DCI

State	Output Voltage Level	Switching Sequence					
		S1	S2	S3	S4	S5	S6
1	$2V_{dc}$	ON	ON	ON	OFF	OFF	OFF
2	V_{dc}	OFF	ON	ON	OFF	OFF	OFF
3	*0*	OFF	OFF	ON	OFF	OFF	OFF
4	$-V_{dc}$	OFF	OFF	OFF	ON	ON	OFF
5	$-2V_{dc}$	OFF	OFF	OFF	ON	ON	ON
6	*0*	OFF	OFF	OFF	ON	OFF	OFF

A. Mathematical Modelling of PV cell

PV array comprises of series and parallel combination of PV panels. These panels are further made up of PV cells. Fig. 3 shows the equivalent circuit of a PV cell, where, i_{ph} is the photon current, i_D is diode current representing the voltage dependent current lost to recombination, i_{pv} is the current available at the cell terminals, V_{pv} is the terminal voltage,$r_s$and r_p are the series and shunt resistances, respectively [3]. The relationship between i_{ph}, i_D, i_{pv} and v_{pv} can be stated as [3]

$$i_{pv} = i_{ph} - i_D - \frac{V_{pv}+r_s.i_{pv}}{r_p} \quad (1)$$

Further, i_D can be represented as [3]

$$i_D = i_{sat}.\left[e^{q.(V_{pv}+r_s.I_{pv})/A.k.T} - 1\right] \quad (2)$$

where, i_{sat} is the diode saturation current, q is the electrical charge, A is the diode ideality factor, k is the Boltzmann constant, and T is the temperature.

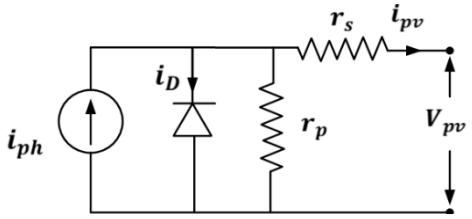

Fig. 3. Electrical equivalent circuit of single PV cell [3].

B. Modelling of battery system

Due to its low cost, rechargeable lead-acid battery is still preferred for higher capacity. The terminal voltage of the battery can be mathematically expressed as in (3), where V_{bt} and E_{cell} are the terminal voltage and internal cell voltage of the battery, and I_b is the current supplied by the battery, R_{int} is the internal resistance of the battery. While discharging, $E_{cell} > V_{bt}$ (as there is a voltage drop across the internal resistance of the battery) and $I_b > 0$ (as current is being supplied by the battery), whereas during charging, $I_b < 0$ (as the current is flowing into the battery from the charger) and $V_{bt} > E_{cell}$ (as the charging current causes voltage drop across the internal resistance of the battery). As

stated in [17], E_{cell} is nonlinear and function of state-of-charge (SOC) of the battery, I_b and low frequency current dynamics.

$$V_{bt} = E_{cell} - I_b R_{int} \tag{3}$$

C. Modelling of 5-level DCI

5-level DCI has output voltage levels namely, zero, $\pm V_{dc}$, and $\pm 2V_{dc}$. The relationship between the switching state, output voltage and switching sequence is shown in Table I. Based on this, the mathematical model of 5-level DCI is as given in (4), where V_{out} is a 1x1 matrix representing the output voltage of 5-level DCI, X is a 1×6 matrix representing the state, S is 6×6 matrix representing switching sequence, U is 6×1 matrix representing the input *dc* voltages of the 5-level DCI (i.e. V_{dc1}, V_{dc2}, V_{dc3}, V_{dc4}).

$$[V_{out}] = [X]_{1\times 6} \times [S]_{6\times 6} \times [U]_{6\times 1} \tag{4}$$

Equation (4) can be further expanded and represented as,

$$[V_{out}] = \begin{bmatrix} x_1 \\ x_2 \\ x_3 \\ x_4 \\ x_5 \\ x_6 \end{bmatrix}^T \begin{bmatrix} T_1 & T_2 & T_3 & T_4 & T_5 & T_6 \\ T_1 & T_2 & T_3 & T_4 & T_5 & T_6 \\ T_1 & T_2 & T_3 & T_4 & T_5 & T_6 \\ T_1 & T_2 & T_3 & T_4 & T_5 & T_6 \\ T_1 & T_2 & T_3 & T_4 & T_5 & T_6 \\ T_1 & T_2 & T_3 & T_4 & T_5 & T_6 \end{bmatrix} \begin{bmatrix} V_{dc1} \\ V_{dc2} \\ 0 \\ 0 \\ V_{dc3} \\ V_{dc4} \end{bmatrix} \tag{5}$$

Where,
x_i=1 for ith state else, x_i=0 zero for any other state
T_i =1 if S_i is ON and T_i =0 if S_i is off, for i =1 to 6

Considering $V_{dc1}=V_{dc2}=V_{dc3}=V_{dc4}=V_{dc}$, (5) can be simplified as

$$[V_{out}] = \begin{bmatrix} x_1 \\ x_2 \\ x_3 \\ x_4 \\ x_5 \\ x_6 \end{bmatrix}^T \begin{bmatrix} 2V_{dc} \\ V_{dc} \\ 0 \\ 0 \\ -V_{dc} \\ -2V_{dc} \end{bmatrix} \tag{6}$$

Therefore, for State-1 x_1=1 and x_2-x_6 are zero. Hence, $V_{out} = 2V_{dc}$. Similarly, different output voltage levels can be obtained corresponding to the switching state being employed.

IV. Operating Modes Of Standalone Microgrid

The proposed microgrid incorporates HGS interfaced with the *ac* loads through 5-level DCI. Depending on the load demand, atmospheric conditions and generation capability, different sources come into picture over the daily operation and full cycle of the *ac* supply. This section presents discussion on the operation of the proposed standalone micorgrid under five different operating modes, as defined in Table II, in the following subsections. During the Mode I–IV, the AVR controls the excitation of DG_1 and DG_2 to regulate V_{dc1}–V_{dc4} at V_{dc}.

A. MODE-I

This mode is related to periods of high light intensity and considers that the power generated by PV and DG exactly match the load demand. This infers that the battery pack has no role to play in this mode. The battery pack is idle and takes no part in power transfer in terms of charging or discharging. The duty cycle of *dc-dc* converters, interfacing PV_1 and PV_2 with the respective *dc*-links, are controlled to ensure that V_{dc2} and V_{dc3} regulated at V_{dc}.

B. MODE-II

In this mode, along with the DGs and PVs, B_1 and B_2 also supply power to meet the load demand. This mode comes into effect when due to the low irradiance levels, the PV_1 and PV_2 cannot solely maintain V_{dc2} and V_{dc3}, respectively. Hence, in order to meet the load demand the bidirectional *dc-dc* converters operate as boost converter to control the discharging of B_1 and B_2. The combination of PV_1–B_1 and PV_2–B_2 supply the necessary power to (i) regulate V_{dc2} and V_{dc3} at V_{dc}, and (ii) meet the load demand with the help of DG_1 and DG_2.

C. MODE-III

When operating in Mode I or II, if the load is considerably reduced then the excess power would result in loss of regulation for V_{dc2}–V_{dc3}. Mode–III can solve this issue by changing the operation of bidirectional converters from boot to buck mode and facilitating the charging of B_1–B_2. Thus, the battery act as load and excess power generated by PV_1 and PV_2 are utilized for controlled battery charging. This charging action ensures that V_{dc2}–V_{dc3} are maintained at V_{dc}, while ensuring that the light load demand is met. The charged battery can be used to support the load demand in case of Mode–II and IV.

D. MODE-IV

If B_1 and B_2 have sufficient charge, then at night or in absence of solar irradiance, they can support the load. B_1 and B_2 need to be charged during the daytime by operating the system in Mode–III. B_1 and B_2 will discharge accordingly as in Mode–II and regulate V_{dc2}–V_{dc3} at V_{dc}.

E. MODE-V

Under no-load condition or if DG is unavailable due to maintenance requirement or some other issue, then the ac load is not supplied with electric power. If this occurs at night time or during the periods of low light intensity then PV_1 and PV_2 do not produce enough power for any sort of

TABLE II. Different Operating Modes Of Proposed Standalone 5-level DCI Based Microgrid

Operating Modes	Energy Source						Energy Consumption		
	DG_1	$PVES_1$		$PVES_2$		DG_2	Load	B_1	B_2
		PV_1	B_1	PV_2	B_2				
MODE-I	YES	YES	NO	YES	NO	YES	YES	NO	NO
MODE-II	YES	YES	YES	YES	YES	YES	YES	NO	NO
MODE-III	YES	YES	NO	YES	NO	YES	YES	YES	YES
MODE-IV	YES	NO	YES	NO	YES	YES	YES	NO	NO
MODE-V	NO	YES	NO	YES	NO	NO	NO	YES	YES

utilization. However, in such a scenario arises during day time then the generated electric energy available at the terminals of PV_1 and PV_2 can be utilized to charge B_1 and B_2, respectively. Depending on the load demand, battery and atmospheric conditions, one of the five modes can be activated.

TABLE III. PERFORMANCE OF THE STANDALONE MICROGRID WITH 5-LEVEL DCI BASED HGS

Operating Modes	Load (Ω)	Load Current (A)	Power Supplied (W)						Power Consumed (W)		
			DG_1	$PVES_1$		$PVES_2$		DG_2	Load	B_1	B_2
				PV_1	B_1	PV_2	B_2				
MODE-II	15	9	237	158	223	158	227	246	1249	-	-
MODE-III	26	5.22	143	402	-	402	-	145	750	172	170
MODE-IV	20	6.75	182	0	288	0	290	187	947	-	-

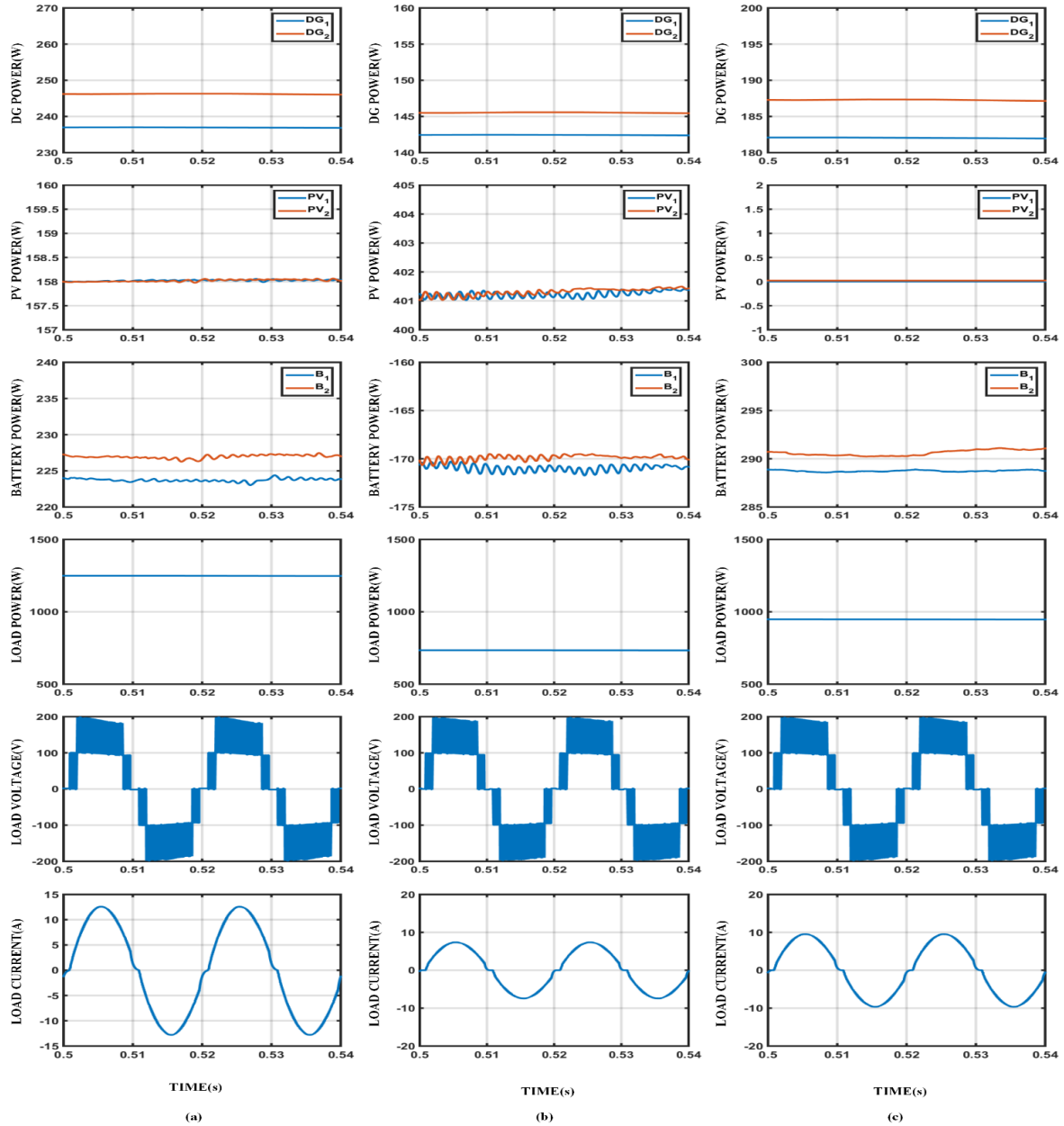

Fig. 4. (a) DG power, PV power, Battery pack power, Load power, Load voltage and Load current operating in Mode II,
(b) DG power, PV power, Battery pack power, Load power, Load voltage and Load current operating in Mode III, and
(c) DG power, PV power, Battery pack power, Load power, Load voltage and Load current operating in Mode IV.

V. SIMULATION RESULTS

The proposed standalone microgrid with 5-level DCI based HGS is modeled on MATLAB/SIMULINK platform. The specifications of each energy source and storage element is given in Appendix. The energy conversion efficiency of the PV panels is low, which necessitates the need of maximum power point tracking (MPPT) to extract maximum

power under the existing environmental conditions [3]. Incremental Conductance (IC) method is an attractive MPPT technique based on instantaneous conductance of the PV array, which is computationally simple and easy to implement [18]. In this work, IC MPPT technique is employed to extract the maximum power from the PV array. Also, V_{dc1}–V_{dc2}–V_{dc3}–V_{dc4} are regulated at 100V. The 5-level DCI, operated with multi-carrier pulse width modulation technique, has the peak output voltage of 200V. The performance of proposed standalone microgrid architecture for operating modes II–IV, discussed in the following sub-sections, is tabulated in Table - III.

A. MODE-II

Fig. 4 (a) shows the steady state performance of the standalone microgrid with 5-level DCI based HGS operating under Mode-II. The load demand is 1249W and power available from PV_1–PV_2 and DG_1–DG_2 are 316W and 483W, respectively. This cannot meet the load demand and hence, B_1–B_2 are subjected to controlled discharging so as to and provide 450W to meet the load demand. The total harmonic distortion of load current (THD) is 4.33%.

B. MODE-III

Similarly, the steady state performance of the proposed standalone microgrid operating under Mode-III is shown in Fig. 4 (b). The load demand is 750W and power available from PV_1–PV_2 and DG_1–DG_2 are 804W and 288W, respectively. The power generation exceeds the load demand. This excess power can be utilized to charge the battery packs. Hence, in this mode B_1–B_2 are operate under controlled charging so as to and store excess 342W. This stored energy can be utilized when the generated power is lesser than the demand, as in case of Mode–II and IV. THD of the load current is 4.85%.

C. MODE-IV

Fig. 4 (c) shows the steady state performance of the proposed standalone microgrid operating under Mode–IV. As this mode involves the periods of low light intensity and night time, the PV power is unavailable. When the load demand is 947W and power available from PV_1–PV_2 and DG_1–DG_2 are 0W and 369W, respectively. To meet the load demand, B_1–B_2 provide the stored energy during Mode – III to the load through the bidirectional *dc-dc* converter and DCI. The battery operates in discharging mode to supply 578W to meet the load demand. THD of the load current is 4.77%.

VI. CONCLUSIONS

In this paper, standalone microgrid with 5-level DCI using HGS is reported and modelled on MATLAB/SIMULINK platform. The system performance is analyzed for different modes. The presence of 5-level DCI in the proposed standalone microgrid architecture ensures that the output current THD is within the 5% limit. For the PV arrays, the use of IC algorithm ensures the extraction of maximum PV power. The battery packs operate in charging and discharging mode depending on whether the PV power and DG can meet the load demand or not. In Mode–III, the battery pack is charged whereas in Mode – II and IV, the battery pack discharges. The system reliability and self-sustenance capability are enhanced with the incorporation of DGs in HGS. These advantages do not burden the system with the need of synchronization or fundamental current extraction associated with DGs incorporated in standalone microgrids. This is an added advantage along with the merits of less component, system higher efficiency and decreased voltage stress on switches, renders the proposed scheme as an attractive alternative for rural electrification.

REFERENCES

[1] B. Blackstone, C. Hicks, O. Gonzalez and Y. Baghzouz, "Improved islanded operation of a diesel generator — PV microgrid with advanced inverter," *2017 IEEE 26th International Symposium on Industrial Electronics (ISIE)*, Edinburgh, 2017, pp. 123-127.

[2] J. Hurtt, D. Jhirad and J. Lewis, "Solar resource model for rural microgrids in India," *2014 IEEE PES General Meeting | Conference & Exposition*, National Harbor, MD, 2014, pp. 1-5.

[3] A. V. Sant, V. Khadkikar, W. Xiao, H. Zeineldin and A. Al-Hinai, "Adaptive control of grid connected photovoltaic inverter for maximum VA utilization," *IECON 2013 - 39th Annual Conference of the IEEE Industrial Electronics Society*, Vienna, 2013, pp. 388-393.

[4] K. C. Patel, A. V. Sant and M. H. Gohil, "Shunt active filtering with NARX feedback neural networks based reference current generation," *2017 International Conference on Power and Embedded Drive Control (ICPEDC)*, Chennai, 2017, pp. 280-285

[5] K. Kant, C. Jain and B. Singh, "A Hybrid Diesel-WindPV-Based Energy Generation System With Brushless Generators," in *IEEE Transactions on Industrial Informatics*, vol. 13, no. 4, pp. 1714-1722, Aug. 2017.

[6] J. G. de Matos, F. S. F. e Silva and L. A. d. S. Ribeiro, "Power Control in AC Isolated Microgrids With Renewable Energy Sources and Energy Storage Systems," in IEEE Transactions on Industrial Electronics, vol. 62, no. 6, pp. 3490-3498, June 2015.

[7] Shatakshi, B. Singh and S. Mishra, "Dual mode operational control of single stage PV-battery based microgrid," 2018 IEEMA Engineer Infinite Conference (eTechNxT), New Delhi, 2018, pp. 1-5.

[8] H. Mahmood, D. Michaelson and J. Jiang, "A Power Management Strategy for PV/Battery Hybrid Systems in Islanded Microgrids," in IEEE Journal of Emerging and Selected Topics in Power Electronics, vol. 2, no. 4, pp. 870-882, Dec. 2014.

[9] H. Nehrir *et al.*, "A review of hybrid renewable/alternative energy systems for electric power generation: Configurations, control and applications," *2012 IEEE Power and Energy Society General Meeting*, San Diego, CA, 2012, pp. 1-1.

[10] J. Sachs and O. Sawodny, "A Two-Stage Model Predictive Control Strategy for Economic Diesel-PV-Battery Island Microgrid Operation in Rural Areas," in IEEE Transactions on Sustainable Energy, vol. 7, no. 3, pp. 903-913, July 2016.

[11] P. Sanjeev, N. P. Padhy and P. Agarwal, "A novel configuration for PV-battery-DG integrated standalone DC microgrid," 2018 International Conference on Power, Instrumentation, Control and Computing (PICC), Thrissur, 2018, pp. 1-6.

[12] Shatakshi, Ikhlaq, B. Singh and S. Mishra, "A synchronous generator based diesel-PV hybric micro-grid with power quality controller," 2017 IEEE 26th International Symposium on Industrial Electronics (ISIE), Edinburgh, 2017, pp. 952-956.

[13] J. Rodriguez, Jih-Sheng Lai and Fang Zheng Peng, "Multilevel inverters: a survey of topologies, controls, and applications," in *IEEE Transactions on Industrial Electronics*, vol. 49, no. 4, pp. 724-738, Aug. 2002.

[14] J. Rodriguez, S. Bernet, P. K. Steimer and I. E. Lizama, "A Survey on Neutral-Point-Clamped Inverters," in *IEEE Transactions on Industrial Electronics*, vol. 57, no. 7, pp. 2219-2230, July 2010.

[15] J. Selvaraj and N. A. Rahim, "Multilevel Inverter For Grid-Connected PV System Employing Digital PI Controller," in *IEEE Transactions on Industrial Electronics*, vol. 56, no. 1, pp. 149-158, Jan. 2009.

[16] X. Guo, M. C. Cavalcanti, A. M. Farias and J. M. Guerrero, "Single-Carrier Modulation for Neutral-Point-Clamped Inverters in Three-Phase Transformerless Photovoltaic Systems," in *IEEE Transactions on Power Electronics*, vol. 28, no. 6, pp. 2635-2637, June 2013.

[17] MathWorks, (2018). Simscape/Simulink/SimPowerSystems Toolbox: Battery (R2018b). Retrieved Nov. 30, 2018. From https://in.mathworks.com/help/physmod/sps/powersys/ref/battery.html

[18] M. A. Elgendy, B. Zahawi and D. J. Atkinson, "Assessment of the Incremental Conductance Maximum Power Point Tracking Algorithm," in *IEEE Transactions on Sustainable Energy*, vol. 4, no. 1, pp. 108-117, Jan. 2013.

APPENDIX

Specifications:

DG_1/DG_2: 1-phase, 50Hz, 500VA, 70.7V; **PV_1/PV_2:** open-circuit voltage: 106.75V, short-circuit current: 6.3A, maximum power under STC**:** 500W; **B_1/B_2:** 72V, 7Ah.